

A Coupled Physical–Biological Pelagic Model of a Shallow Sill Fjord

Dag L. Aksnes and Ulf Lie

*Department of Fisheries and Marine Biology, University of Bergen,
Thormøhlens gt. 55, 5008 Bergen, Norway*

Received 19 December 1989 and in revised form 9 May 1990

Keywords: numerical model; meteorological control; stratification; vertical distribution; nutrients; plankton; fjord; Norway

A vertically resolved model for the land-locked fjord Lindåspollene, western Norway is presented. Salinity, temperature, oxygen, nitrogen-nutrients, silicate, and two groups of phytoplankton and herbivores are represented as dynamic variables. From 'below' the model is driven by solar radiation, precipitation, wind and tidal exchange and from 'above' by herbivore mortality. Simulation results are presented and discussed together with actual observations from Lindåspollene. The main seasonal and vertical characteristics of the phytoplankton and herbivore dynamics seem to be well reflected by the model, and realistic seasonal patterns may be produced for several successive years. The most characteristic vertical features are the formation of a summer surface production maximum and a deep chlorophyll maximum. Furthermore, a herbivore biomass which develops in the surface layer divides into a shallow and a deep component during summer and becomes concentrated in the surface layer again in the autumn. The nutricline and the pycnocline develop independently of one another, with consequences for the supply of nutrients to the upper euphotic zone. The bottom-up control exerted by the meteorological forcing, especially the freshwater runoff, seems to be of paramount significance for the observed vertical structure and seasonality of the present fjord system.

Introduction

The land-locked fjord, Lindåspollene (Figure 1), has a property in common with lakes in that only narrow entrances connect it with the outside fjord system. Hence, the open boundary problems are reduced to a minimum, which makes the pelagic compartment of such a system amenable to ecological research and modelling. Although the physical forcing differs from the usual ocean ecosystem, the biological processes and even the species composition are similar to nearby coastal and oceanic systems. Accordingly, Lindåspollene was selected as the locality for studies of ecological processes governing the population dynamics of the local herring stock (Dahl *et al.*, 1973). Since 1969, many published and unpublished (mainly thesis work) ecological field studies have been carried out at the herring level (Lie *et al.*, 1978; Johannessen, 1983), and at the lower levels of the ecosystem (Lännergren, 1975, 1976, 1978; Lännergren & Skjoldal, 1975; Skjoldal & Lännergren, 1978; Lie *et al.*, 1983; Aksnes & Magnesen, 1983; Skjoldal *et al.*, 1983;

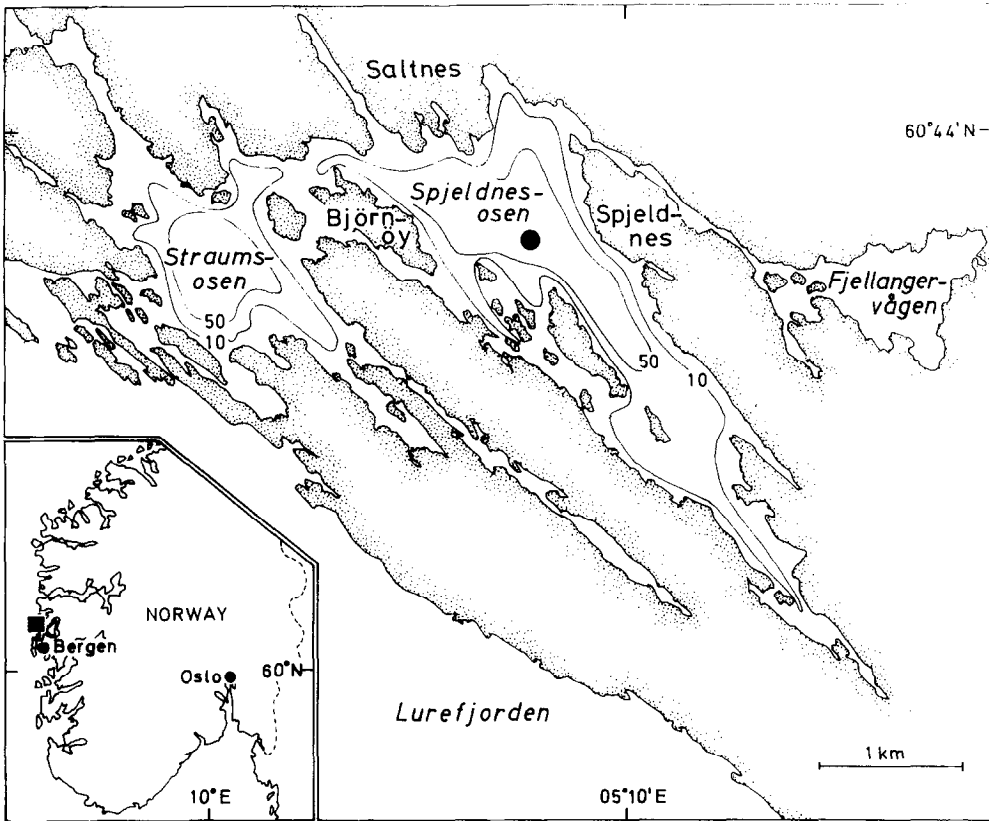


Figure 1. Map of Lindåspollene. ●, indicates the deepest location (89 m). Measurements presented in Figures 5 and 6 have been obtained at this location.

Wassmann, 1983; Aksnes *et al.*, 1985; Skjoldal & Wassmann, 1986; Aksnes & Magnesen, 1988; Magnesen, 1988; Magnesen *et al.*, 1989*a,b*). Here, we report on a model based upon these studies which is designed to encompass the major physical forcing functions and processes responsible for the formation of pelagic primary and secondary biomass. It includes a dynamical time–depth representation of physical, chemical and biological state variables and processes.

In recent years there has been much discussion about the role of nutrients supplied by domestic sewage, runoff from agriculture or acid rain in coastal waters. The watermasses of fjords with shallow sills are typically strongly stratified during summer and generally believed to be oligotrophic as a result of decreased turbulent mixing and low nutrient supply from below. The nutrient content of the freshwater, however, may be an important source of new nutrients. In order to test this, the model was run with normal freshwater input, but with the nutrient content of the freshwater set to zero. This simulation gives rise to a discussion of the significance of freshwater nutrients for the magnitude and the vertical structure of primary and secondary production.

The model

Temperature, salinity, oxygen and nutrients (silica and nitrogen) are the physical/chemical state variables of the model, while the biological state variables are represented

TABLE 1. Forcing variables, state variables and boundary specifications (t is time and z is depth)

| | Symbol | Unit |
|--|----------------------|--|
| <i>Forcing variables</i> | | |
| Incident radiation | $L(t)$ | Langley h^{-1} |
| Freshwater runoff | $R(t)$ | m water h^{-1} |
| Wind | $W(t)$ | cm s^{-1} |
| Tide | u_0 | m h^{-1} |
| <i>State variables</i> | | |
| Salinity | $S(t,z)$ | ‰ |
| Temperature | $T(t,z)$ | $^{\circ}\text{C}$ |
| Oxygen | $O(t,z)$ | $\text{l O}_2 \text{m}^{-3}$ |
| Nitrogen-nutrients | $N(t,z)$ | $\text{mg-at nitrogen m}^{-3}$ |
| Silicate | $Si(t,z)$ | $\text{mg-at silica m}^{-3}$ |
| Diatoms | $D(t,z)$ | $\text{mg chlorophyll } a \text{ m}^{-3}$ |
| Flagellates | $F(t,z)$ | $\text{mg chlorophyll } a \text{ m}^{-3}$ |
| 'Surface layer' herbivores depth integrated | $H1(t,z)$ $S1(t)$ | mg carbon m^{-3} mg carbon m^{-3} |
| 'Chlorophyll maximum' herbivores depth integrated | $H2(t,z)$ $S2(t)$ | mg carbon m^{-3} mg carbon m^{-3} |
| Herbivore faeces | $Fe(t,z)$ | mg carbon m^{-3} |
| Density | $G(t,z)$ | kg m^{-3} |
| Static stability | $E(t,z)$ | m^{-1} |
| Light | $I(t,z)$ | Langley h^{-1} |
| Turbulent diffusion | $K(t,z)$ | $\text{m}^2 \text{h}^{-1}$ |
| Vertical current due to tide | $w_v(t,z)$ | m h^{-1} |
| 'Horizontal' current due to tide | $u(t,z)$ | m h^{-1} |
| <i>Boundary specifications</i> | | |
| Temperature of runoff water | $T_A(t)$ | $^{\circ}\text{C}$ |
| N-nutrients of runoff water | $N_A(t)$ | $\text{mg-at nitrogen m}^{-3}$ |
| Silicate of runoff water | $Si_A(t)$ | $\text{mg-at silica m}^{-3}$ |
| Temperature of incoming tide | $T_B(t)$ | $^{\circ}\text{C}$ |
| Salinity of incoming tide | $S_B(t)$ | ‰ |
| Oxygen of incoming tide | $O_B(t)$ | $\text{l O}_2 \text{m}^{-3}$ |
| N-nutrients of incoming tide | $N_B(t)$ | $\text{mg-at nitrogen m}^{-3}$ |
| Silicate of incoming tide | $Si_B(t)$ | $\text{mg-at silica m}^{-3}$ |
| Diatoms of incoming tide | $D_B(t)$ | $\text{mg chlorophyll } a \text{ m}^{-3}$ |
| Flagellates of incoming tide | $F_B(t)$ | $\text{mg chlorophyll } a \text{ m}^{-3}$ |

by two phytoplankton groups, two herbivorous groups and one group representing the faecal matter of the herbivores (Table 1). The common currency of the biomass is nitrogen, and conversions between nitrogen, chlorophyll a and carbon are made by constants.

The forcing functions of the model (Table 1) are surface radiation, freshwater runoff, wind and tidal advection (including the water characteristics of the incoming tide). The differential equations are listed in Table 2, while the physical and biological processes (Table 3) will be subsequently explained. Actual parameter values used in the present runs are given in Table 4.

Tide

The inflowing tide is introduced at the depth where the density of the water column is equal to the density of the tidal inflow. The characteristics of this inflow are specified as

TABLE 2. The differential equations. Explanation to the symbols are given in Tables 3 and 4. u' and R' are tidal exchange and freshwater supply expressed instantaneously

Salinity

$$\frac{\delta S}{\delta t} = -w \frac{\delta S}{\delta z} - u'(S - S_B) + \frac{\delta}{\delta z} K \frac{\delta S}{\delta z} - R' S$$

Temperature

$$\frac{\delta T}{\delta t} = -w \frac{\delta T}{\delta z} - u'(T - T_B) + \frac{\delta}{\delta z} K \frac{\delta T}{\delta z} - R'(T - T_A) + c_1 I$$

Oxygen

$$\frac{\delta O}{\delta t} = -w \frac{\delta O}{\delta z} - u'(O - O_B) + \frac{\delta}{\delta z} K \frac{\delta O}{\delta z} + c_2(P_1 + P_2 - R_1 - R_2 - R_3 - R_4 - R_5)$$

N-nutrients

$$\frac{\delta N}{\delta t} = -w \frac{\delta N}{\delta z} - u'(N - N_B) + \frac{\delta}{\delta z} K \frac{\delta N}{\delta z} + R' N_A - c_3(P_1 + P_2 - R_1 - R_2 - R_3 - R_4 - R_5)$$

Silicate

$$\frac{\delta Si}{\delta t} = -w \frac{\delta Si}{\delta z} - u'(Si - Si_B) + \frac{\delta}{\delta z} K \frac{\delta Si}{\delta z} + R' S_A - c_4 P_1$$

Diatoms

$$\frac{\delta D}{\delta t} = -(w + s_1) \frac{\delta D}{\delta z} - u'(D - D_B) + \frac{\delta}{\delta z} K \frac{\delta D}{\delta z} + c_5(P_1 - R_1 - G_1 - G_2)$$

Flagellates

$$\frac{\delta F}{\delta t} = -(w + s_2) \frac{\delta F}{\delta z} - u'(F - F_B) + \frac{\delta}{\delta z} K \frac{\delta F}{\delta z} + c_5(P_2 - R_2 - G_3 - G_4)$$

'Surface layer' herbivores (integrated for the entire water column)

$$\frac{dS_1}{dt} = \int P_3 dz - \int R_3 dz - M_1 S_1$$

'Chlorophyll-maximum' herbivores (integrated)

$$\frac{dS_2}{dt} = \int P_4 dz - \int R_4 dz - M_2 S_2$$

Faecal pellets

$$\frac{\delta Fe}{\delta t} = -(w + s_3) \frac{\delta Fe}{\delta z} + K \frac{\delta^2 Fe}{\delta z^2} + k_2(P_5 - R_5)$$

boundary conditions (Table 1). Due to the shallow sill of Lindåspollene (3 m), the outflowing tide is always let out in the upper depth cell (0–2 m).

Incident radiation

The incident radiation was based on hourly measurements from the period 1970–78 obtained from publications of the Geophysical Institute, University of Bergen. A combined exponential–cosine function was fitted to these measurements and incorporated in the model.

Precipitation

Precipitation is represented by daily measurements obtained at Lindås. The runoff to Lindåspollene was estimated by multiplying the precipitation (represented as a 6-day running mean) with the ratio between the runoff area and the area of the poll. To compensate for evaporation, this runoff was reduced by a factor of 0.5 in the period from 15 May–

TABLE 3. Biological processes

| Process | Symbol | Unit |
|---------------------------------------|------------|--|
| Gross production of diatoms | $P_1(t,z)$ | mg carbon m ³ h ⁻¹ |
| Respiration of diatoms | $R_1(t,z)$ | mg carbon m ³ h ⁻¹ |
| Grazing of diatoms by herbivore 1 | $G_1(t,z)$ | mg carbon m ³ h ⁻¹ |
| Grazing of diatoms by herbivore 2 | $G_2(t,z)$ | mg carbon m ³ h ⁻¹ |
| Sinking rate of diatoms | $s_1(t,z)$ | m h ⁻¹ |
| Gross production of flagellates | $P_2(t,z)$ | mg carbon m ³ h ⁻¹ |
| Respiration of flagellates | $R_2(t,z)$ | mg carbon m ³ h ⁻¹ |
| Grazing of flagellates by herbivore 1 | $G_3(t,z)$ | mg carbon m ³ h ⁻¹ |
| Grazing of flagellates by herbivore 2 | $G_4(t,z)$ | mg carbon m ³ h ⁻¹ |
| Sinking rate of flagellates | s_2 | m h ⁻¹ |
| Gross production of herbivore 1 | $P_3(t,z)$ | mg carbon m ³ h ⁻¹ |
| Respiration of herbivore 1 | $R_3(t,z)$ | mg carbon m ³ h ⁻¹ |
| Mortality of herbivore 1 | $M_1(t)$ | h ⁻¹ |
| Mean depth of herbivore 1 | m_1 | m |
| Gross production of herbivore 2 | $P_4(t,z)$ | mg carbon m ³ h ⁻¹ |
| Respiration of herbivore 2 | $R_4(t,z)$ | mg carbon m ³ h ⁻¹ |
| Mortality of herbivore 2 | $M_2(t)$ | h ⁻¹ |
| Mean depth of herbivore 2 | $m_2(t,z)$ | m |
| Production of faecal pellets | $P_5(t,z)$ | mg carbon m ³ h ⁻¹ |
| Decomposition of faecal pellets | $R_5(t,z)$ | mg carbon m ³ h ⁻¹ |
| Sinking rate of faecal pellets | s_5 | m h ⁻¹ |

15 September. The nutrient content of the runoff water was represented by measurements carried out by Magnesen *et al.* (1989b).

Wind

Wind speeds exceeding a certain velocity influence the turbulent diffusion of the water column (see below). Wind speeds were obtained from measurements made at Bergen airport, located about 50 km south of Lindåspollene.

Turbulent diffusion

Turbulent diffusion (K) is influenced by the dissipation rate of turbulent kinetic energy (e) and the buoyancy frequency (N) according to the empirical expression (Denman & Gargett, 1983)

$$K = 0.25eN^{-2} \quad (1)$$

where

$$N^2 = (g/r) (dr/dz) \quad (2)$$

g is the acceleration due to gravity, r is the density, and dr/dz is the vertical density gradient. Density was calculated from the state variables, salinity (S) and temperature (T). Aure (1972) has calculated turbulent diffusion for different periods and depth layers in Lindåspollene. Using his data we calculated an average e_A for the top layer, and used this value as a minimum ($e_A = 4.4 \cdot 10^{-8} \text{ m}^2 \text{ s}^{-3}$). Higher values of e_A were calculated from the actual wind strength (W , m s^{-1})

$$e_A = a_1 W^3 + a_2 \quad (3)$$

where a_1 and a_2 are constants. Estimates of these constants were obtained from a linear regression fitted to the measurements of e at wind speeds of 5 and 15 m s^{-1} (given in Table

TABLE 4. Parameter values

| Parameter | Explanation | Value |
|-----------|--|--|
| u_0 | Tidal velocity | m h^{-1} |
| w_0 | Deep water pumping rate | $8.33 \cdot 10^{-2} \text{ m h}^{-1}$ |
| a_1 | Wind/dissipation relation | $4.9 \cdot 10^{-9} \text{ m}^{-1}$ |
| a_2 | Wind/dissipation relation | $4.23 \cdot 10^{-8} \text{ m}^2 \text{ s}^{-3}$ |
| a_3 | PAR correction and surface loss | 0.25 |
| a_4 | Extinction due to water | 0.04 m^{-1} |
| a_5 | Extinction due to non-chlorophyll | 0.10 m^{-1} |
| a_6 | Extinction due to chlorophyll | $1.38 \cdot 10^{-2} \text{ mg}^{-1} \text{ m}^{-1}$ |
| a_7 | Pmax at 0 °C, diatoms | $4.81 \text{ C chlorophyll}^{-1} \text{ h}^{-1}$ |
| a_8 | Temperature dependence, Pmax-diatoms | $6.71 \cdot 10^{-2} \text{ }^\circ\text{C}^{-1}$ |
| a_9 | Pmax at 0 °C, flagellates | $2.67 \text{ C chlorophyll}^{-1} \text{ h}^{-1}$ |
| a_{10} | Temp. dependence, Pmax-flagellates | $1.29 \cdot 10^{-1} \text{ }^\circ\text{C}^{-1}$ |
| a_{11} | Respiration rate at 0 °C, phytoplankton | $2.9 \cdot 10^{-3} \text{ h}^{-1}$ |
| a_{12} | Respiration rate temperature dependence | $0.07 \text{ }^\circ\text{C}^{-1}$ |
| a_{13} | Maximum ration at 0 °C, herbivores | $1.04 \cdot 10^{-2} \text{ h}^{-1}$ |
| a_{14} | Maximum ration temperature dependence | $1.36 \cdot 10^{-1} \text{ }^\circ\text{C}^{-1}$ |
| a_{15} | Ivlev constant | $7.00 \cdot 10^{-3} \text{ m}^3 (\text{mg C})^{-1}$ |
| a_{16} | Assimilation efficiency, herbivores | 0.8 |
| a_{17} | Reduced winter metabolism (1.11–1.2) | 0.2 |
| a_{18} | Respiration rate at 0 °C, herbivores | $4.17 \cdot 10^{-3} \text{ h}^{-1}$ |
| a_{19} | Respiration rate temperature dependence | $6.93 \cdot 10^{-2} \text{ }^\circ\text{C}^{-1}$ |
| a_{20} | Density dependent mortality parameter | $2.3 \cdot 10^{-6} \text{ m}^2 \text{ mg}^{-1} \text{ h}^{-1}$ |
| a_{21} | Density dependent mortality parameter | $4.58 \cdot 10^{-4} \text{ h}^{-1}$ |
| a_{22} | Density dependent mortality parameter | $4.17 \cdot 10^{-2} \text{ h}^{-1}$ |
| a_{23} | Decomposition rate of faecal pellets | $3.33 \cdot 10^{-2} \text{ h}^{-1}$ |
| k_1 | Half saturation nitrogen, diatoms | 0.1 mg-at m^{-3} |
| k_2 | Half saturation silicate, diatoms | 1.0 mg-at m^{-3} |
| k_3 | Half saturation nitrogen, flagellates | 0.1 mg-at m^{-3} |
| c_1 | Heat/radiation conversion | $1.0 \cdot 10^{-6} \text{ }^\circ\text{C cal}^{-1}$ |
| c_2 | l oxygen/mg carbon ratio | $1.87 \cdot 10^{-3} \text{ l mg}^{-1}$ |
| c_3 | mg-at nitrogen/mg carbon ratio | $1.19 \cdot 10^{-2} \text{ mg-at mg}^{-1}$ |
| c_5 | mg chlorophyll <i>a</i> /mg carbon ratio | $3.33 \cdot 10^{-2} \text{ mg mg}^{-1}$ |
| d_1 | Vertical range parameter, herbivore 1 | 3.0 |
| d_2 | Vertical range parameter, herbivore 2 | 5.0 |
| m_1 | Mean depth of herbivore 1 | 2.0 |
| s_2 | Sinking rate of flagellates | 0.01 m h^{-1} |
| s_3 | Sinking rate of faecal pellets | 2.08 m h^{-1} |
| I_1 | Lower limit, Iopt | 4.5 |
| I_2 | Upper limit, Iopt | 8.0 |

1 of Denman and Gargett, 1983). Aure (1972) found, on average, that the $e_B/e_A = 0.03$, where e_B is the dissipation below the pycnocline of Lindåspollene. We have used this relationship to calculate e_B . The depth specific $e(z)$ was calculated by assuming a linear decrease in the top layer and a constant value for the deep layer (but varying with time). The depth specific turbulent diffusion, $K(z)$ was then calculated as

$$K(t, z) = 0.25 e(t, z) N(t, z)^{-2}. \quad (4)$$

At each time step an exact positioning between the top and the bottom layer was determined as the depth with the highest density gradient between 10 and 20 m depth.

Light

The light (I) at depth z (which is positive) was calculated as

$$I(z,t) = a_3 R(t) e^{-k} \quad (5a)$$

where

$$k = a_4 z + a_5 z + a_6 \int_0^z (D(t,z) + F(t,z)) dz \quad (5b)$$

where $R(t)$ is the surface radiation, a_3 converts incident radiation to photosynthetically active radiation and corrects for loss through the surface film. The a_4 , a_5 and a_6 are the attenuation constants due to seawater, non-chlorophyll materials and chlorophyll. Thus, self-shading from phytoplankton is included.

Primary production

The relationship between phytoplankton production and light is represented by the equation of Steele (1962), while the nutrient uptake is represented by Michaelis-Menten kinetics

$$P_1(t,z) = P_{\max}(t,z) \frac{I(t,z)}{I_{\text{opt}}} e^{(1-I(t,z)/I_{\text{opt}})} N_{\text{lim}} D(t,z) \quad (6a)$$

where,

$$N_{\text{lim}} = \min(l_1, l_2), \quad l_1 = \frac{N(t,z)}{k_1 + N(t,z)}, \quad l_2 = \frac{\text{Si}(t,z)}{k_2 + \text{Si}(t,z)}. \quad (6b)$$

Silicate is not considered limiting for the flagellates. P_{\max} [$C(\text{chlorophyll } a)^{-1} \text{ h}^{-1}$], which is the production under optimal light (I_{opt}) and without nutrient limitation, was made temperature dependent as suggested by Eppley (1972). We have chosen the relation

$$P_{\max}(t,z) = a_7 e^{a_8 T(t,z)}. \quad (7)$$

This expression refers to the diatoms, while the flagellate parameters are termed a_9 and a_{10} . The maximum value of P_{\max} was set equal to $15 C$ ($\text{chlorophyll } a)^{-1} \text{ h}^{-1}$ for both groups. I_{opt} was set equal to the light level in the upper 2 m, but was not allowed to vary outside the interval $I_1 \dots I_2$ (Table 4).

Sinking rate

The sinking rate of the flagellates (s_2) is set constant, while the diatom sinking rate (s_1) is a function of the ambient concentration of the nitrogen-nutrients $N(t,z)$. The minimum value of s_1 was 0.5 m day^{-1} [when $N(t,z) > 5 \text{ g—at N m}^{-3}$], and the maximum value was 2 m day^{-1} [when $N(t,z) = 0 \text{ g—at N m}^{-3}$]. Interpolation was made to obtain values between the extremes.

Respiration and decomposition

The respiration and decomposition of diatoms and flagellates were assumed to be related to the temperature, $T(t,z)$, in accordance with the equation

$$R_1(t,z) = c_5^{-1} a_{11} D(t,z) e^{a_{12} T(t,z)}. \quad (8)$$

Vertical distribution of the herbivores

Herbivore group 1 was restricted to the surface layer, while herbivore group 2 was assumed to concentrate at the chlorophyll a maximum. The surface association of the first

group was selected according to observations that indicate the existence of a non-migrant mesozooplankton group close to the surface (Aksnes & Magnesen, 1988; Magnesen *et al.*, 1989a).

The depth distribution of the herbivorous biomass was computed according to Aksnes and Magnesen (1988)

$$H1(t, z) = S1(t)[g(z) + g(-z) + g(2z_{\text{crit}} - z)] \quad (9)$$

where $S1(t)$ is the depth-integrated biomass. The g -function is the normal frequency distribution with mean m and standard deviation d (Table 4). With the above equation no biomass is allowed to be distributed above the surface or below the depth z_{crit} . This last depth represents a limitation due to anoxic conditions or on reaching the bottom. The mean depth of the herbivores was not allowed to go below those with an oxygen concentration of less than 2 ml l^{-1} . If the depth of the maximum phytoplankton concentration is far from the surface and z_{crit} , the vertical distribution of herbivore group 2 will be approximately normally distributed around the depth of the phytoplankton maximum. The mean depth of herbivore 1 (m_1 in Table 4) was set time invariant. Depth standard deviations (d_1 , d_2) were selected according to observations made in Lindåspollene.

The vertical distribution was computed for each time step. It was routinely ensured that no biomass was lost or gained from one time step to another as a result of the division of the water column into 2-m depth cells.

Zooplankton feeding

The zooplankton feeding is represented in a similar fashion as that proposed by Kremer and Nixon (1978). The ration ingested is obtained from a maximum ration (temperature dependent), which is reduced by food-density dependent limitation and competition from dense biomass. In the present runs we have assumed equal preference for diatoms and flagellates by both herbivore groups. The maximum ration r_{max} (h^{-1}), is given as a function of temperature (Kremer & Nixon, 1978)

$$r_{\text{max}}(t, z) = a_{13}e^{a_{14}T(t, z)}. \quad (10)$$

The realized ration (r_r , $\text{mg C m}^{-3} \text{ h}^{-1}$) was obtained by first calculating an estimated ration (r_e , $\text{mg C m}^{-3} \text{ h}^{-1}$), and then an instantaneous filtering rate (F_i , h^{-1}) (Kremer & Nixon, 1978)

$$r_e = H1(t, z)r_{\text{max}}c_5^{-1}B(1 - e^{a_{15}c_5^{-1}B}) \quad (11a)$$

$$F_i = \frac{r_e}{c_5^{-1}B} \quad (11b)$$

$$r_r = c_5^{-1}B(1 - e^{-F_i}) \quad (11c)$$

where B is the biomass of both diatoms and flagellates,

$$B = D(t, z) + F(t, z).$$

Assimilation efficiency

The assimilation efficiency was assumed constant (a_{16}) for both herbivore groups and gross growth was expressed as

$$P_3(t, z) = a_{16}r_r. \quad (12)$$

Faecal production

Faecal production was defined as the unassimilated matter

$$P_5(t, z) = (1 - a_{16})r_r. \quad (13)$$

Losses due to metabolism

Losses due to metabolism were expressed as a temperature dependent power function (both groups):

$$R_3(t, z) = H1(t, z)a_{17}a_{18}e^{a_{19}(t, z)}. \quad (14)$$

The parameter a_{17} has a value of 1 except during winter. Reduced winter metabolism as observed by Hirche (1983) and Båmstedt and Tande (1988) is represented by this parameter (Table 4).

Herbivore mortality

The herbivore mortality was expressed as an empirical density dependent function operating on the total (depth integrated) biomass ($S1$ and $S2$):

$$\begin{aligned} M_1(t, z) &= 0 && \text{when } S1(t) \leq 0.2 \text{ mg C m}^{-2} \\ M_1(t, z) &= (a_{20}S1(t) - a_{21}) && \text{when } 0.2 < S1(t) < 2 \\ M_1(t, z) &= a_{22} && \text{when } S1(t) \geq 2. \end{aligned} \quad (15)$$

This relation was used for both herbivorous groups. The empirical constants were derived from mortality estimates obtained from mesozooplankton in Lindåspollene (Hassel, 1980; Aksnes & Magnesen, 1983, 1988).

Decomposition of faecal material

The decomposition of faecal material was computed according to

$$R_5(t, z) = a_{23}Fe(t, z) \quad (16)$$

and the sinking rate of this material was given as a constant (s_3).

Numerical solution

The finite difference scheme included a first order scheme for the local change of the state variables, upwind differencing for the advective (including sinking) terms (Press *et al.*, 1987, p. 630), an explicit scheme for the diffusive terms (Wroblewski, 1983), and a Euler approximation of the biological terms. Vertical grid spacing was 2 m, and the time step was 0.5 h. The turbulent diffusion coefficient [$K(t, z)$] was not allowed to exceed $1 \text{ m}^2 \text{ h}^{-1}$ in order to achieve numerical stability. The nitrogen mass balance was routinely checked during each run. Initial values and boundary conditions were supplied from measurements conducted over several years (using averaging and interpolation). One-year simulation took about 15 min with an IBM-3090 with vector facility. This execution time may, however, be greatly reduced by more efficient programming.

Results of model simulations and earlier studies

The time solutions for the state variables are given in Figures 2, 3 and 4. At four selected dates (21 January, 1 April, 1 July and 1 October) we have also presented the simulation

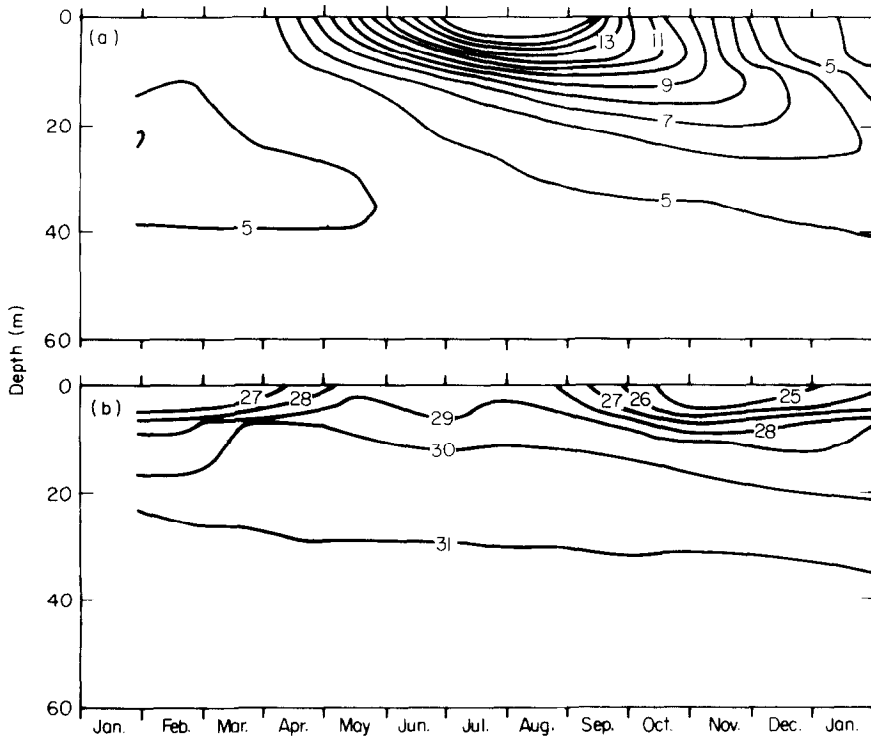


Figure 2. (a) Simulated temperature ($^{\circ}\text{C}$) and (b) salinity (‰) distributions.

results as vertical profiles together with actual measurements indicated as shaded areas (Figures 5 and 6). The shaded areas indicate the minimum and maximum values of earlier published (Lännergren, 1975, 1976, 1978; Lännergren & Skjoldal, 1975; Skjoldal & Lännergren, 1978; Lie *et al.*, 1983; Skjoldal *et al.*, 1983; Aksnes *et al.*, 1985; Skjoldal & Wassmann, 1986; Magnesen, 1988) and unpublished records (1972–84) made in Lindåspollene. The zooplankton observations are based on the data of Magnesen (1988) obtained by Clarke–Bumpus samplers equipped with a mesh size of $60\ \mu\text{m}$. These data cannot be directly compared with our model results. While a herbivore is accurately defined and identified in a model it is not so in nature. Therefore, the y -axis for the zooplankton in Figure 6 represents the percentage of the total biomass rather than absolute values.

Winter and spring

Saline stratification and exchange of deep water. Until late April the temperature is rather homogeneous ($4\text{--}5\ ^{\circ}\text{C}$) in the entire water column (Figure 2). The distribution of salinity, however, indicates a stratification of the water masses in January. In some years this stratification may disappear and a salinity close to 31–32 appears in the entire water column (April, Figure 5). The mechanism for this destratification is an increase in the salinity of the top layer associated with reduced land runoff due to cold winter/spring periods and/or reduced precipitation. Such meteorological conditions may trigger a renewal of the deep water of the pool. No such renewal occurred during the first spring in

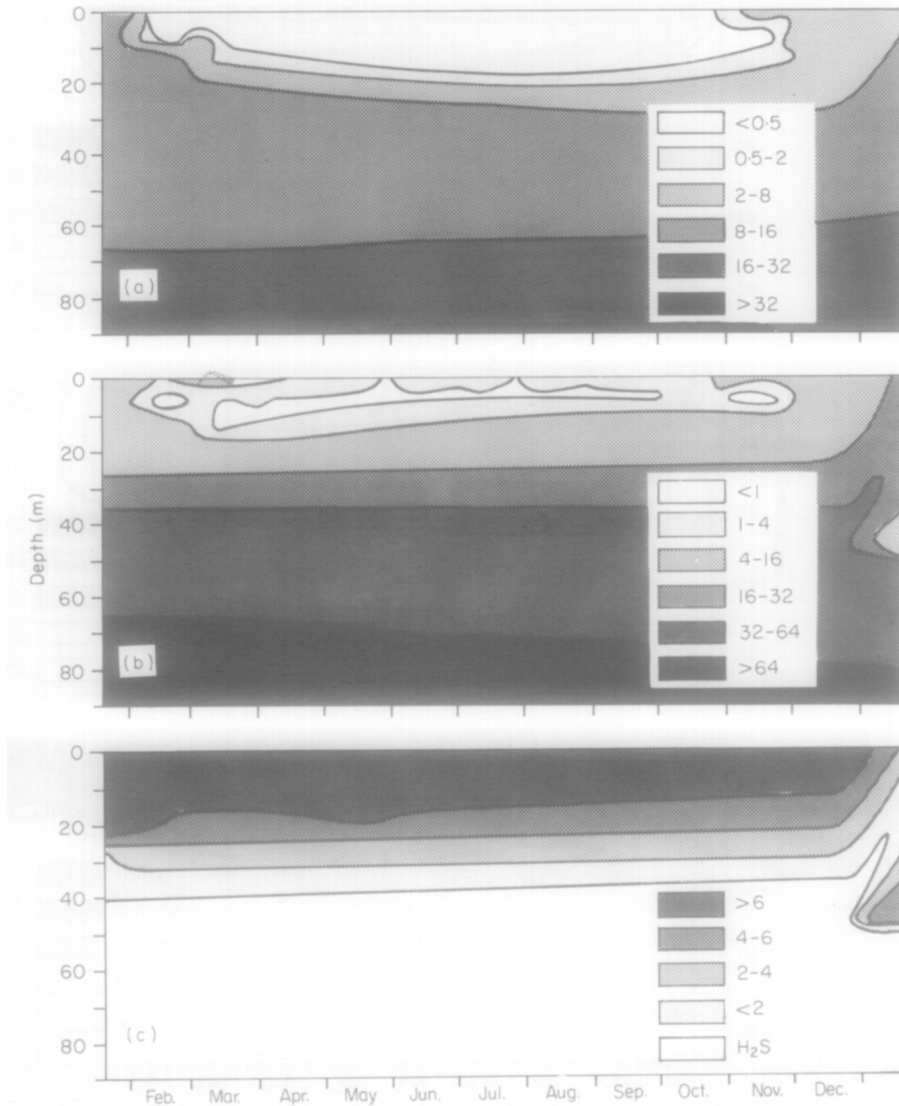


Figure 3. Simulated distribution of (a) N-nutrients (mM), (b) silicate (mM), and (c) oxygen (ml l^{-1}) distributions.

the present simulation, but it could be provoked by a slight increase in the salinity of the incoming tide. The present simulation shows the initiation of an intermediate renewal during the next January (oxygen, Figure 3).

Spring bloom. The most conspicuous difference between the simulation and the observations of phytoplankton productivity in Lindåspollene is the time of occurrence of the spring bloom. Several observations (Lännergren, 1975, 1976; Lännergren & Skjoldal, 1975; Lännergren, 1978; Skjoldal & Wassmann, 1986) indicate that the bloom culminates during March, whereas our model gives maximum bloom in the middle of February (Figure 4). It is conceivable that the initial phytoplankton concentration in the model was

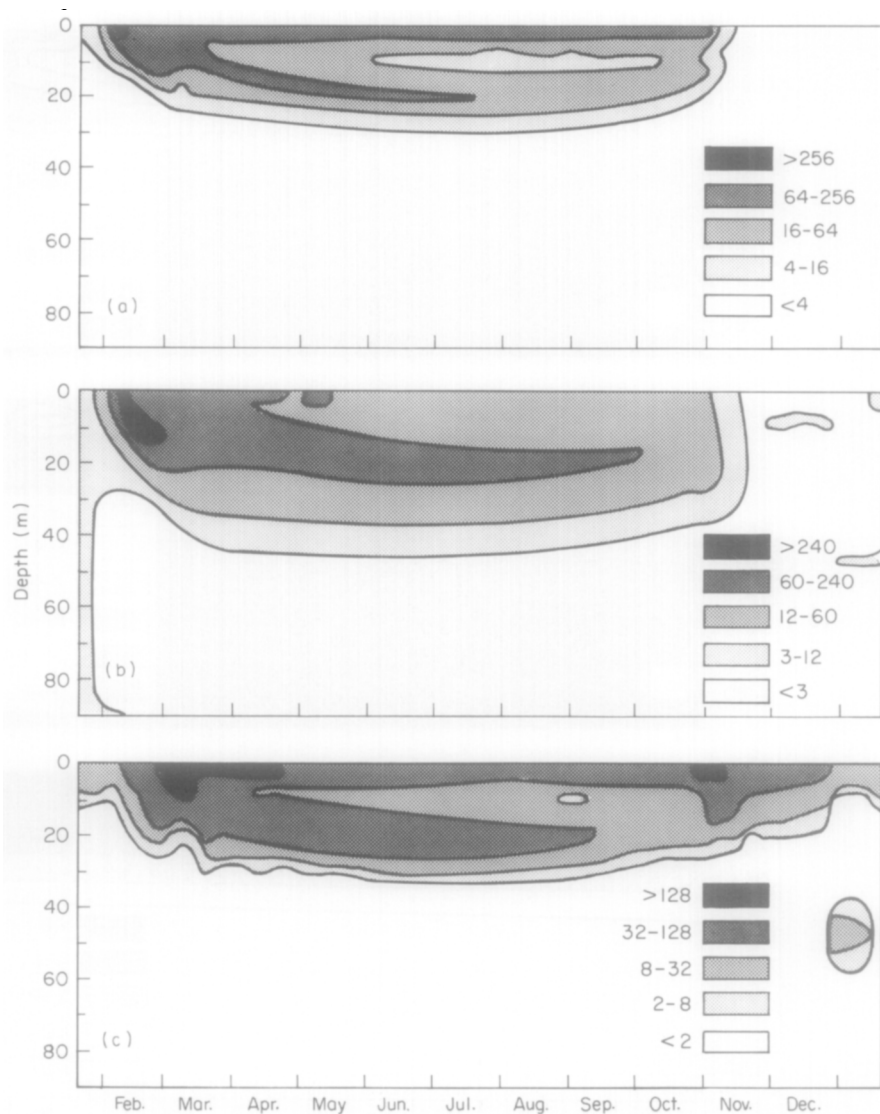


Figure 4. (a) Simulated primary production ($\text{mg C m}^{-3} \text{ day}^{-1}$), (b) phytoplankton biomass (mg C m^{-3}) and (c) herbivore biomass (mg C m^{-3}).

too high ($0.1 \text{ mg chlorophyll m}^{-3}$ for both diatoms and flagellates), but reducing this by a factor of 10 only delayed the date for maximum spring bloom from 17 to 27 February (Table 5). Ice cover, however, is a characteristic feature in the major part of Lindåspollene during winter, but is not included in the simulation presented in Figures 3–6. Ice cover, particularly when there is snow on the ice, can significantly reduce the photosynthetically available radiation (PAR), and hence the primary production. Simulating ice cover by reducing the PAR to 40% of the basic run (Table 5) resulted in a delay of the maximum spring bloom until 23 March. Increased cloud cover will, of course, have a similar effect on the reduction of PAR.

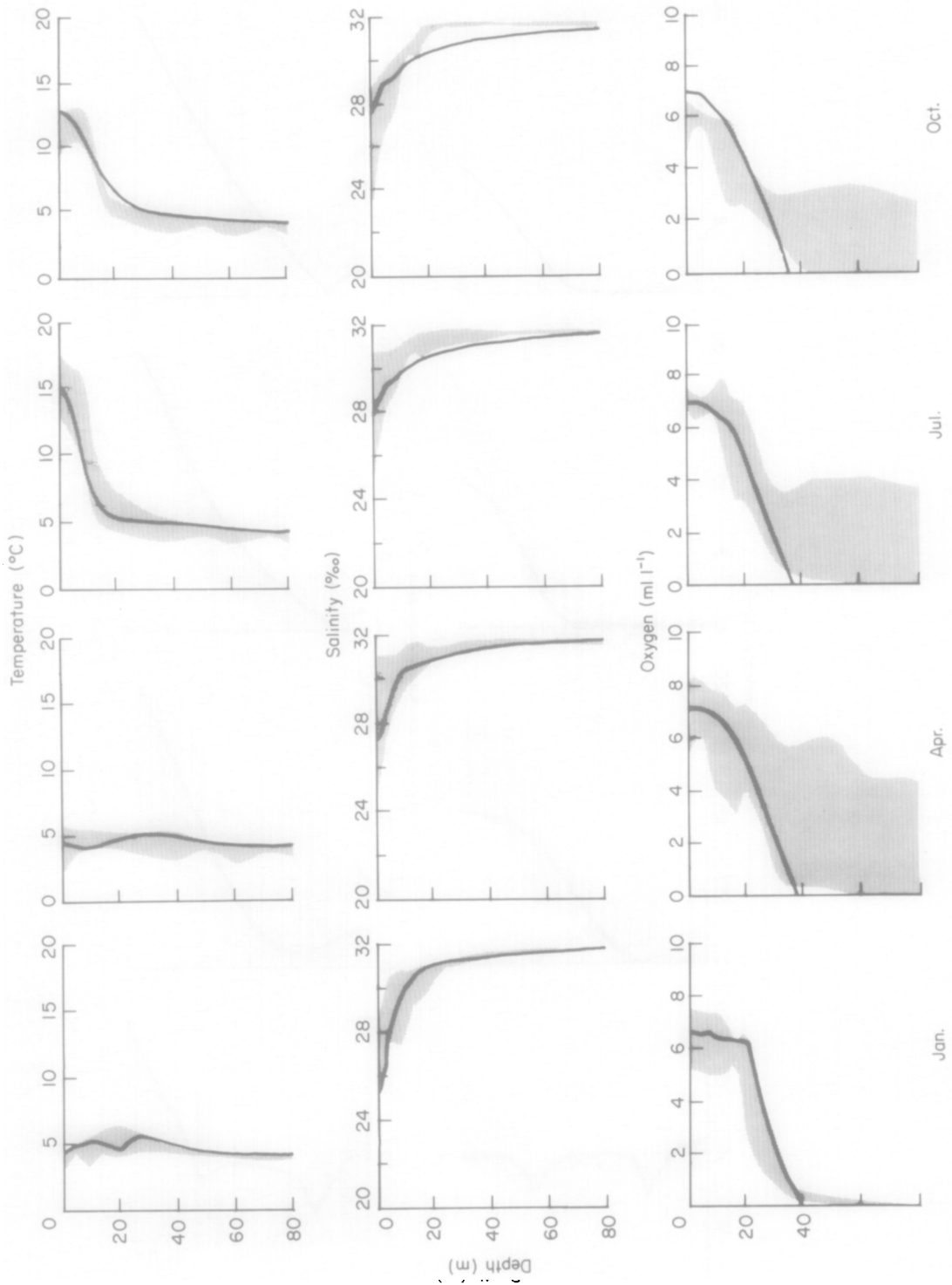
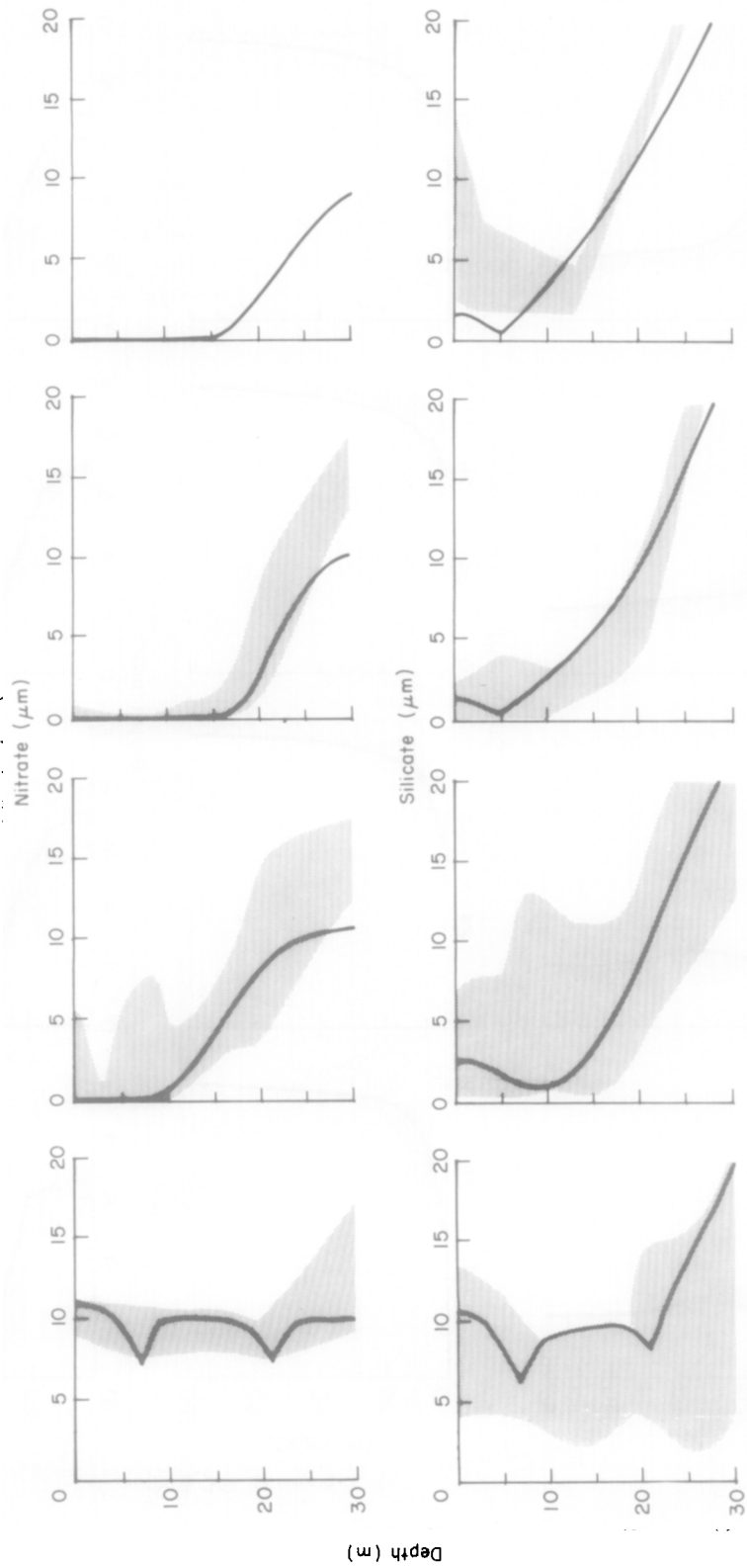


Figure 5. Simulated (—) and observed (---) vertical distribution at four selected dates (see text for explanation).



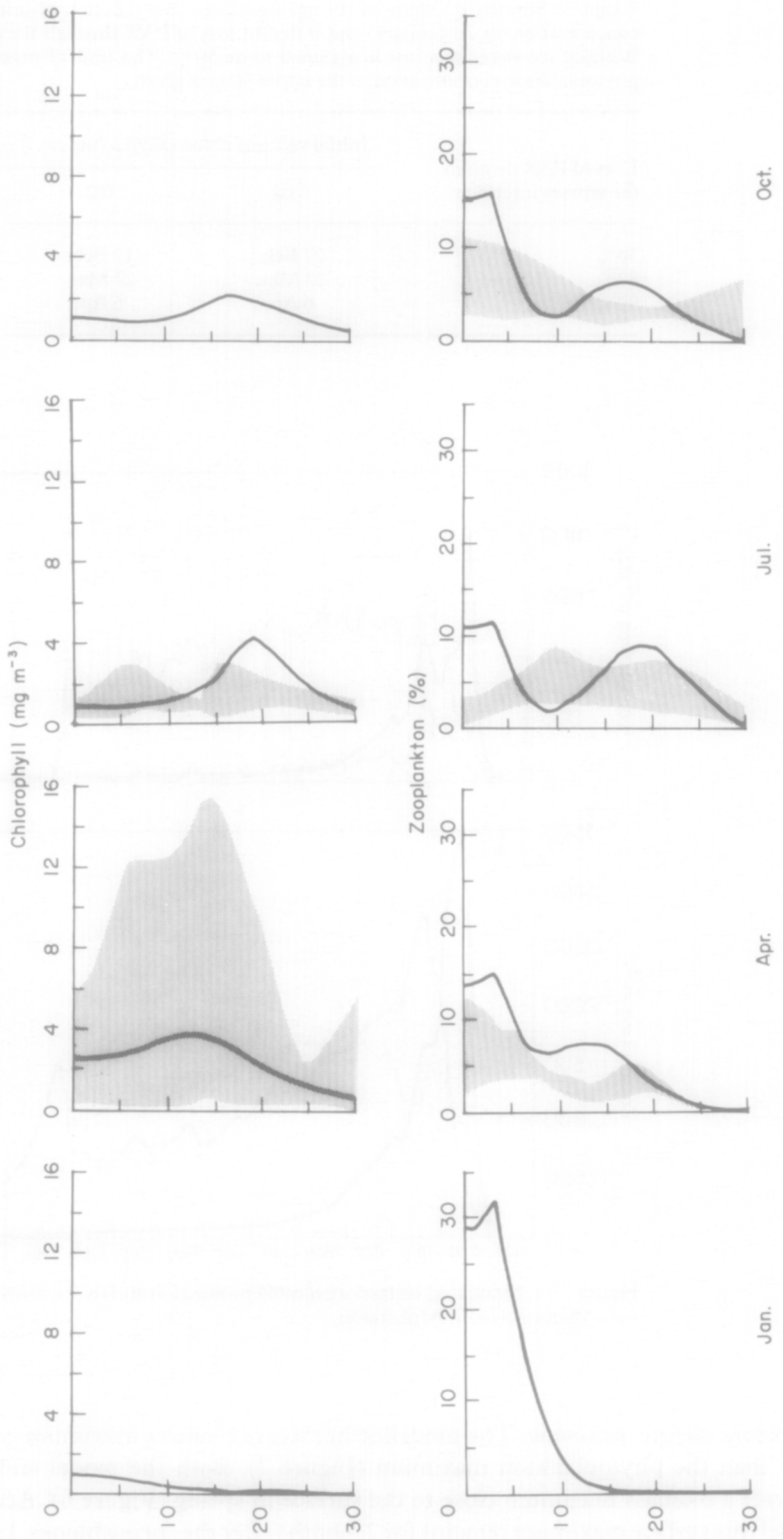


Figure 6 Simulated (---) and observed (—) vertical distribution at four selected dates (see text for explanation).

TABLE 5. Simulated timing of the spring bloom as a function of initial chlorophyll *a* concentration (at 20 January) and different loss of PAR through the air-sea interface. Without ice-cover this loss is assumed to be 50%. The time of maximum integrated phytoplankton concentration in the upper 30 m is given

| Loss of PAR through the air-sea interface | Initial value of chlorophyll <i>a</i> (mg m ⁻³) | |
|---|---|---------|
| | 0.02 | 0.2 |
| 50% | 27 Feb. | 17 Feb. |
| 80% | 23 Mar. | 22 Mar. |
| 90% | 6 Apr. | 6 Apr. |

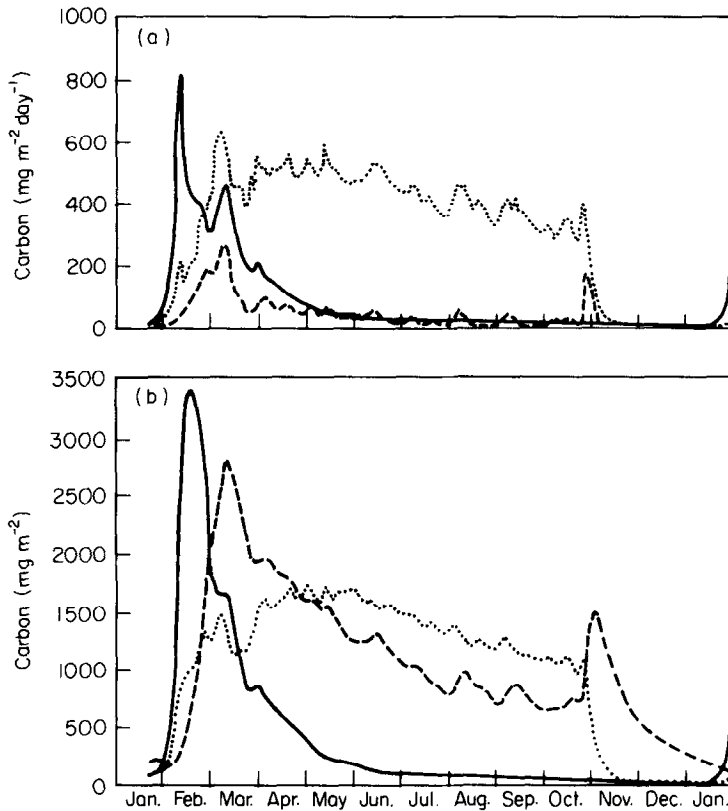


Figure 7. (a) Simulated surface-integrated production and (b) biomass. ····, flagellates; —, diatoms; ---, zooplankton.

Herbivore surface maximum. The modelled herbivore biomass maximum occurs 1 month later than the phytoplankton maximum (Figure 7). Both the model and observations indicate a biomass maximum close to the surface in spring (Figure 6). According to the model this surface maximum remains for 2 months after the spring bloom. Later in spring,

herbivore group 2 leaves the surface layer and penetrates deeper as the chlorophyll *a* maximum occurs gradually deeper, while herbivore group 1 is forced to remain in the surface layer (see model description).

Summer

Nutrient supply and primary production. A strong thermal stratification develops (Figure 2) as a result of increased local solar input and tidal exchange of thermal energy. The land runoff also preserves a haline stratification, although not so strong as in January. The July nutricline is located below 20 m (Figure 6), and is about 10 m deeper than the thermo- and pycnocline. Thus, the primary production above the pycnocline is nutrient limited, while the production below the pycnocline is both nutrient and light limited. Hence, the new production during summer is controlled mainly by three factors: (1) the light availability in the deep nutrient-rich water, which depends on the intensity of solar radiation and the turbidity of the water, (2) the turbulent diffusion of nutrients within the watermasses below the pycnocline, and (3) the nutrients supplied with freshwater runoff to the layer above the pycnocline. The diffusion of nutrients across the pycnocline is probably of minor importance as the nutricline is located deeper than the pycnocline. The model predicted primary production during summer was in the range of 400–500 mg C m⁻² day⁻¹ (Figure 7). From June to September Lännergren (1976) reported a ¹⁴C-fixation rate of 48.2 g C m⁻² corresponding to a daily rate of about 400 mg C m⁻². Both observations (Lännergren, 1976, 1978; Skjoldal *et al.*, 1983; Aksnes *et al.*, 1985) and the model indicate a production maximum in the upper 5 m. The model predicts another production maximum associated with the nutricline (Figure 4). This has not been reflected in ¹⁴C-fixation measurements, except for measurements undertaken in spring (April–March, Lännergren, 1976). Most ¹⁴C-fixation measurements undertaken during summer, however, have been carried out at depths above the nutricline. Support for photosynthetic activity at the base of the nutricline, however, is given by observations of chlorophyll *a* maxima at this depth. Skjoldal and Wassmann (1986) described a more or less marked, although, consistent deep chlorophyll *a* maximum during summer. Also Erga (1990) reports values in the range of 2–5 mg chlorophyll *a* m⁻³ between 20 and 30 m in June. The light is limiting at these depths, and photosynthetic activity is probably intimately coupled to the variations in cloudiness and water turbidity.

Herbivores. The surface integrated herbivore biomass corresponded to 1–2 g C m⁻² and declined during the summer months (Figure 7). The model reflects two depths of herbivore biomass during summer. The first is associated with the surface primary production maximum, while the second is associated with the deep chlorophyll *a* maximum (Figure 4). The modelled deep herbivorous biomass maximum is supported by observations, while the predicted surface maximum seems to be over-estimated by the model (Figure 6). This bias may partly be a result of the depth independent mortality representation used in the model. Visual predation is especially likely to increase the mortality of the more light-exposed surface plankton. A light dependent mortality has also some empirical support since Aksnes and Magnesen (1988) found that the mortality of the surface living *Paracalanus parvus* was about two times higher than the mortality of *Temora longicornis* and *Pseudocalanus elongatus* which lived about 10 m deeper than *P. parvus*.

On the basis of the species composition a two-layered, practically non-migrating zooplankton community was found by Magnesen *et al.* (1989a). In the upper 5 m they

found appendicularians, *Acartia* spp., *P. parvus* and *Centropages hamatus*, while *T. longicornis*, *P. elongatus*, *Oithona similis* and *Oncaea* spp. predominated below this depth. As the present simulation suggests, the vertical zonation of the biomass and the species composition were remarkably constant over the 1-month study period (Aksnes & Magnesen, 1988; Magnesen *et al.*, 1989a).

Autumn and early winter

Nutricline and pycnocline. While the density stratification extends increasingly deeper until October (Figure 2), the nutricline (both nitrate and silicate) becomes gradually shallower (Figure 3). This independence between the nutricline and the pycnocline is supported by the observations (Figures 5 and 6). During late autumn the thermal stratification is reduced, but the haline stratification remains. (Figure 5.)

Nutrient enrichment in the upper layer. During late autumn the surface layer is enriched with nutrients from three sources: an increased freshwater runoff (which is normal in western Norway during autumn), an increasing nutrient level in the incoming tide, and a rising nutricline within the pool. Our model suggests that the nutrients of the deeper water are brought up by tidal displacement rather than by mixing alone. Tidal inflow of dense water intrudes at a depth with a high nutrient content, and these nutrients are thereby convected upwards. The result of this process is seen as increased nitrate and silicate levels in the upper 20 m during December and January (Figure 3). Increased oxygen and reduced silicate concentrations at the depth of tidal intrusion are also a result of this process (Figure 3). The discontinuities in the observed vertical profiles of silicate and nitrate used as initial values (January, Figure 6) give empirical support for such tidal intrusions. Although less marked, discontinuities are also reflected in the temperature and oxygen profile (Figure 5). Several similar discontinuities in hydrographic and chemical parameters have been observed earlier in Lindåspollene, and the reliability of the measurements have sometimes been questioned (unpubl. data). The model, however, supports the existence of such apparent irregularities, and indicates tidal intrusions as likely mechanisms.

Herbivore biomass increase in the surface layer. In October and November the model predicts an increased biomass in the surface layer (Figure 4). This is partly explained by a shallower chlorophyll *a* maximum and thereby a shallower mean depth for herbivore group 2, but increased runoff associated with precipitation also stimulates new production in the surface layer. An autumnal increase in the zooplankton biomass of the surface layer was observed by Magnesen (1988), although that increase started earlier and was more prolonged. The model predicts the duration of such surface associated herbivore 'blooms' to be heavily influenced by the precipitation regime. By prolonging the autumnal rainfall the herbivore increase is also prolonged (Figure 8). The nutrients supplied with the runoff water enter the surface layer, and in the model these nutrients result in the herbivore biomass maximum occurring close to the surface. Another factor that is not considered in the present model is that decreased surface radiation and increased turbidity are both associated with increased precipitation. Hence, the efficiency of visual planktivores may be severely reduced with a corresponding reduction in the mortality of the herbivores. The autumnal increase in herbivore zooplankton may therefore be triggered by a combination of input of new nutrients and reduced visual predation.

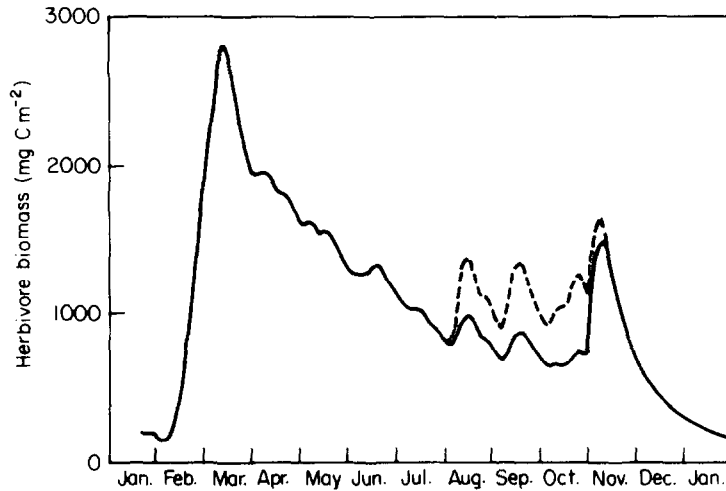


Figure 8. Simulated surface integrated herbivore biomass. ---, indicates a doubling of precipitation in the period August–November.

TABLE 6. Yearly gross production (g C m^{-2}) of phytoplankton and net production of zooplankton in the basic run (A) and in the run with no nutrients in runoff water (B)

| | A | B |
|-------------|------|-----|
| Diatoms | 30 | 24 |
| Flagellates | 115 | 70 |
| Zooplankton | 13.4 | 6.6 |
| | 145 | 94 |

Removal of the nutrients in the runoff water

On an annual basis the effect of removing the nutrients in the freshwater caused a 35% decrease in total phytoplankton production, and a 51% reduction in the herbivore production (Table 6). The change was most prominent during the summer where the surface maximum in primary production and herbivore biomass disappeared when the freshwater nutrients were removed (Figure 9). Thus, the two-layered herbivore structure of the normal simulation is associated with the sources of new nutrients, i.e. the runoff water and the nutricline. Above the pycnocline, the freshwater nutrients seem to be the major source of new nutrients entering as the stratification is strong. The nutricline is located below the pycnocline, and the exchange of organic material through the pycnocline is small due to limited vertical migration (Magnesen *et al.*, 1989a). Our model indicates that about 39% is new and 61% is regenerated production, and nutrients in the runoff water are responsible for about 35% of the new production (Table 7). Our strong emphasis on the role of the freshwater nutrients deviates from earlier interpretations made from field studies (Lännergren, 1978; Skjoldal *et al.*, 1983), and this question will be further addressed in the discussion.

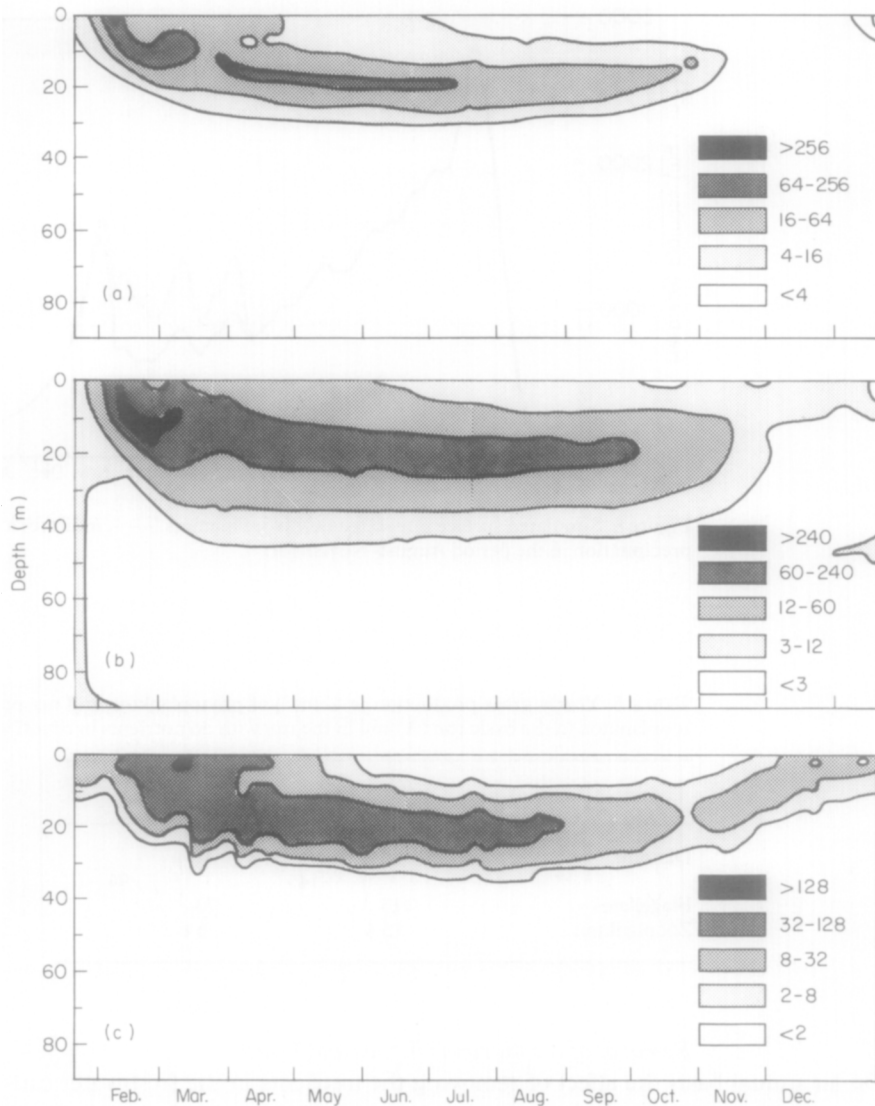


Figure 9. (a) Simulated primary production ($\text{mg C m}^{-3} \text{ day}^{-1}$), (b) phytoplankton biomass (mg C m^{-3}) and (c) herbivore biomass (mg C m^{-3}) when the nutrients in the freshwater runoff are removed.

Simulating several years

During the simulated year, the salinity decreases and the temperature increases in the deep water (Figure 5). This is in accordance with observations and is due to turbulent diffusion. It seems, however, that the model produces too much turbulence as desalination and temperature increases seem to be higher than supported by the observations (Figure 5). The resulting decrease in deep water density increases the probability of a deep water exchange. The model was run for 5 years with the same forcing applied each year, and a résumé of the simulation is given in Table 8. The productivity of the water column was enhanced as an increasingly larger part became oxygenated through spring renewals of the

TABLE 7. The ratio between annual regenerated and new primary production

| | mg C m ⁻² year ⁻¹ | % of total production | % of new production |
|------------------------|---|-----------------------|---------------------|
| New production | | | |
| Freshwater nutrients | 20 | 14 | 35 |
| Marine nutrients | 37 | 25 | 65 |
| Regenerated production | 88 | 61 | |
| Total production | 145 | 100 | |

TABLE 8. Results from a 5-year simulation. Anoxia is indicated by the percentage of the water column that is anoxic in July

| Year | Production (g C m ⁻² year ⁻¹) | | | | Anoxia (%) |
|------|--|-------------|-------|------------|---------------|
| | Diatoms | Flagellates | Total | Herbivores | |
| 1 | 30 | 115 | 145 | 13 | 56 |
| 2 | 43 | 107 | 150 | 14 | 44 |
| 3 | 81 | 91 | 172 | 20 | 44 |
| 4 | 124 | 85 | 209 | 33 | 0 |
| 5 | 97 | 112 | 209 | 34 | 0 |

deep water. The diatom production increased while the flagellate production decreased. This is reasonable as the deep water renewal brings up considerable amounts of silicate. Such a shift in phytoplankton composition is also likely to affect the composition of zooplankton. The present model, however, is not constructed to reflect such changes. Equally important for the development of the zooplankton composition is probably the increase in habitat range due to the oxygenation of the deep part of the fjord.

Discussion

Most earlier published vertically resolved models include physical mixing of nutrients and phytoplankton, phytoplankton sinking, growth (including nutrient and light limitation), self-shading, respiration, grazing and regeneration of nutrients. As most of the process equations of such models are empirical (or semi-empirical) rather than mechanistic, different process representations are used. At the nutrient and phytoplankton level, however, most models are essentially the same as that of Radach and Maier-Reimer (1975), although the actual values of the process parameters differ. The most significant differences between models are probably how they are forced (Table 9). Once a deterministic model is defined and the initial values are selected the observed dynamics of the state variables are essentially sophisticated transformations of the applied forcing. Differences in the number and kind of forcing functions are therefore characteristics that make models fundamentally different. Vertical turbulence, which seems to be the most common factor

TABLE 9. A summary of some of the vertically resolved models published in recent years. F indicates that the variable is used as forcing in the referred model, while a D indicates a dynamical representation. Abbreviations: Win(d); Pre(cipitation) and runoff; Rad(iation); Sal(inity); Tem(perature); Tur(bulence); Oxy(gen); Nut(rients); Phy(toplankton); Her(bivores); Car(nivores)

| Authors | Atmospheric | | | Hydrodynamic | | | Chemical | | Biological | | | Simulated period |
|-----------------------------------|-------------|-----|-----|--------------|-----|-----|----------|-----|------------|-----|-----|------------------|
| | Win | Pre | Rad | Sal | Tem | Tur | Oxy | Nut | Phy | Her | Car | |
| Radach & Maier-Reimer, 1975 | | | F | | | F | | | D | D | F | 90 days |
| Winter <i>et al.</i> , 1975 | | | F | | | | | F | D | F | | 40 days |
| Jamart <i>et al.</i> , 1977, 1979 | | | F | | | F | | D | D | F | | 200 days |
| Fasham <i>et al.</i> , 1983 | | | F | | | F | | D | D | F | | 10 days |
| Slagstad, 1981, 1982 | | | F | | | F | | D | D | D | F | 200 days |
| Taylor <i>et al.</i> , 1986 | | | F | | | F | | D | D | F | | 100 days |
| Stigebrandt & Wulff, 1987 | F | F | F | D | D | D | D | D | D | | | 20 years |
| Riley & Stefan, 1988 | F | F | F | | D | D | D | D | D | F | | — |
| Andersen & Nival, 1988, 1989 | | | F | | F | F | | D | D | D | F | 40 days |
| Present model | F | F | F | D | D | D | D | D | D | D | F | 5 years |

used to force models from 'below', exerts strong control over the vertical fluxes of the passive elements and the input rate of new nutrients to the photic zone. In nature the turbulence is dynamically coupled to the stability and energy input to the water column. In coastal areas the stability conditions, and thereby the turbulence, may be strongly affected by the freshwater input. The significance of freshwater is reinforced by the quantity and composition of nutrients that are associated with it and transported directly into the euphotic zone. Freshwater supply therefore affects the system directly by supply of new nutrients at the top of the photic zone, and indirectly through stability and turbulence at the bottom of the photic zone. In our model we therefore wanted to force the model with the freshwater supply (and wind) rather than by the turbulence itself. A similar approach was used by Stigebrandt and Wulff (1987) and Riley and Stefan (1988), where the turbulence was calculated from a dynamically represented stability which in turn was given by the salinity and temperature distributions.

The forcing from 'above' is usually specified by a 'herbivore grazing pressure function' deduced from observed zooplankton abundances. In this respect the present model and those of Slagstad (1981) and Andersen and Nival (1988) differ from the others listed in Table 9. Here, the herbivores are dynamically represented and the forcing is exerted by herbivore mortality. Realistic forcing is difficult to assess and our approach assumes a simple density dependent mortality function (equation 15) which was based on mortality estimates obtained in Lindåspollene (Aksnes & Magnesen, 1983, 1988).

The swimming ability of the herbivores introduces non-trivial problems. Andersen and Nival (1988) assumed vertical turbulence as the only displacement factor for their

herbivores (salps and copepods). Slagstad (1981) implemented vertical migration for his herbivore representing *Calanus* of the Barents Sea. When light was present he assumed migration towards a light level equal to an individual internal reference level, while random movement was assumed during darkness. Our representation of the herbivore physiology and vertical behaviour is much simpler as our herbivores represent a composite of species (in the size range 100–1000 μm) rather than a particular species. The vertical behaviour of herbivores in the present model is based on a maximization of food intake rather than on optimization between predation risk and food intake, and the sites for new production are then attractive for herbivore localization. During summer, we have seen that the two sites of new production are located close to the surface and below the pycnocline. These findings are discussed in the next two sections. In the last sections the significance of ‘top-down’ control *vs.* ‘bottom-up’ control is commented on.

Deep chlorophyll a maximum (DCM) below the pycnocline

The presence of a DCM in the pycnocline has been the focus of most of the earlier vertically resolved models, as this phenomenon is observed in offshore tropical and subtropical areas and in temperate seas and lakes (Banse, 1988). Both model simulations and observations from Lindåspollene indicate development of a nutricline and DCM more or less independently of the pycnocline, which may be a more general feature of strongly stratified systems. The model and the observations indicated a DCM that moved across the pycnocline during spring and became situated at the nutricline about 10 m below the pycnocline during summer. Hence, it is the light availability and the turbulent diffusion *below* the pycnocline that are critical to the deep new production. This differs from the ‘open-sea’ models where the diffusivity across the pycnocline is the key parameter for new production (Taylor, 1988). The light level below the pycnocline is close to the compensation light level for phytoplankton, and the net carbon fixation rate is therefore very sensitive to the surface light level and the light extinction of the overlying water. The existence of a DCM is therefore sensitive to variations in cloudiness, and to the freshwater runoff influencing the turbidity of the water. Such forcing is highly variable on the west coast of Norway during summer, and it may explain why some field observations indicate a DCM while others do not. The modelled persistence of both the DCM and the rise in primary production at the nutricline are probably reinforced by our smoothed light representation and the use of a time invariant extinction due to non-chlorophyll material.

Surface production maximum under strong stratification—based on new or regenerated nutrients?

Several field studies in Lindåspollene have revealed a pronounced maximum in ^{14}C -fixation close to the surface during summer (Lännergren, 1976; Skjoldal *et al.*, 1983; Aksnes *et al.*, 1985 and unpubl. data). It has been suggested that this maximum is caused by high remineralization of nutrients, while the input of freshwater nutrients is believed to be of less importance. The model indicates that the regenerated production is about 61% of the total production (Table 7). This substantiates the role of remineralization, but the model also indicates that the surface production maximum ceases if the freshwater nutrients are withdrawn (Figure 9). Thus, a hypothesis suggested from the simulation is that remineralization is important for the *magnitude* of the surface production maximum, but that the *existence* of the maximum is due to the nutrients of the runoff water. This hypothesis assumes that the rate of remineralization depends on the standing stock of herbivore

biomass, which again depends on the freshwater nutrients that have been supplied within the lifetimes of the herbivores. A cessation in the supply of new nutrients would therefore result in a gradual decrease in herbivores and thereby in remineralized production. In a mesocosm study, Skjoldal *et al.* (1983) measured the ^{14}C -fixation rate in the natural and two enclosed water columns. The results did indicate a reduction in the surface production within the enclosed water columns. After 11 days there was still a maximum in ^{14}C -fixation close to the surface, but this maximum was only 50% of the surface maximum outside the enclosures.

The model predicts that the nutrients in the runoff water are responsible for about 35% of the total annual primary production. As the freshwater nutrients are supplied to the uppermost metres, it is within the surface layer that these new nutrients stimulate the primary production. The influence of the freshwater nutrients on the productivity above the pycnocline, especially in summer, is obviously much more than the annual depth integrated average of 35%. As indicated by the model (Figure 9 *vs.* Figure 4) we are inclined to believe that the supply of freshwater nutrients determines the productivity and vertical structure of phytoplankton and herbivores, and probably also the species composition above the pycnocline.

The significance of meteorological forcing for the long-term structure in the pelagic compartment

The model simulations and the preceding discussion have already pointed out the importance of including meteorological forcing in order to explain the observed seasonal variations in the present state variables. In this section we will speculate on how short-term meteorological forcing may affect the long-term biological structure of the pelagic compartment. It was demonstrated that exchange of the deep water is likely to happen in spring, when both thermal and haline stratification are most likely to be absent. The haline stratification may disappear in periods of reduced land runoff and/or a coastal northerly wind regime that flushes the surface water out of the fjords in western Norway (Sætre *et al.*, 1988).

Renewal of the deep water in Lindåspollene is likely to bring nutrients up to the surface at a time when light is not seriously limiting. This rate of supply of new nutrients into the euphotic zone, which is limited by the tidal range, may stimulate the phytoplankton bloom considerably. This is reflected by the simulation carried out for several years. Here, we see a four-fold increase in diatom production during the year with complete oxygenation compared to the first year with 56% anoxia in the water column (Table 8). Field studies indicate that the copepod *Calanus finmarchicus* becomes the dominant copepod during years with total or partial deep water renewals (Aksnes & Magnesen, 1983; Magnesen, 1988). If the renewal also leads to 100% oxygenation of the water column, *C. finmarchicus* may survive until the next year (Aksnes & Magnesen, 1983). An increase in the carnivores *Sagitta elegans* and *Aglantha digitale* seems also to be associated with deep water renewals and/or the introduction of *C. finmarchicus* (Lie *et al.*, 1983; Magnesen, 1988). Furthermore, Johannessen (1983) found an increased growth of the local herring population associated with the 'Calanus year'. During years of anoxic bottom water the smaller copepods *Paracalanus parvus*, *Pseudocalanus elongatus* and *Temora longicornis* are dominant. Not only the species composition, but also the vertical migrational pattern seem to vary with the hydrographical state of the fjord. In years with extensive exchange of the deep water, pronounced diel migrations have been observed, while practically none or

only minor migrations have been detected during other years (Lie *et al.*, 1983; Magnesen, 1988; Magnesen *et al.*, 1989a).

Thus, it is conceivable that the occurrence of some cold and/or dry weeks in spring may determine species composition of phytoplankton and zooplankton, diurnal and seasonal vertical migration during the next year or years, and herring growth. This, again, emphasizes the importance of including meteorological forcing in models where the aim is to assess the variability observed in nature. On the other hand, a fully explanatory model must also include the mechanisms responsible for biological responses.

'Top-down' and 'bottom-up' control and future work

The present model is driven by the tide and the three meteorological factors: solar radiation, precipitation and wind. This means that, given the initial and boundary values, the time-depth solutions of the physical, chemical and biological state variables are a result of meteorological dynamics only. Despite this, we conclude that the vertical seasonal patterns in temperature, salinity, oxygen, nitrate, silicate, phytoplankton, primary production and herbivores (although to a lesser extent) correspond extremely well with observed patterns. Although no statistical analyses have been performed, the deviations between the model and the observations are hardly larger than the deviations between the observations themselves. Hence, the predictive ability of the model seems to be as good as that of the data set obtained earlier. Given that the forcing of the model was accurate, we believe that the model could have a greater predictive power, but this remains to be tested. Nevertheless, the present model demonstrates that the meteorological forcing functions, together with a set of rather simple physical and biological process equations, explain much of what is actually observed.

Much attention has been paid to the question of whether aquatic ecosystems are 'controlled from below or above' (e.g. Scavia *et al.*, 1986; Northcote, 1987; Lehmann, 1988; McQueen, 1989). Much of the controversy on this matter has probably been stimulated by the ambiguity of the word 'control' itself. Using this word in a loose sense, an ecosystem is of course controlled from below and above simultaneously. Forcing exerted from below and above differs in units as well as in temporal and spatial scales. Accordingly, there is a need for a framework that combines rather than separates the fundamentally different forcings. Our approach stresses the physical control, but this is not the only control. The process equations and parameter values actually used also exert control over the observed dynamics. Specifically, our density dependent mortality representation used for the herbivores exerts a top-down control for the dynamics observed at the lower levels. This mortality formulation is an empirical simplification that ideally should be replaced by a mechanistic mortality representation including carnivore foraging. Such a mechanistic representation would enable simulations of the effect of carnivore predation on lower levels (for example on phytoplankton) under actual meteorological forcing and appropriate boundary specifications. The relative influence of bottom-up and top-down forcing may then be specifically investigated by simulation.

The realism of complex physical-biological coupled models will always suffer from the weakest component. A detailed biological compartment can hardly compensate for a missing dynamic representation of the physical forcing. Insight may be obtained by assuming a constant environment and taking account of equilibrium situations, but marine systems are often characterized by states of transition rather than by a state of equilibrium. As indicated by the present study such transitions are tightly coupled to alterations in environmental forcing. On the other hand, one cannot expect detailed

biological information from a model that is not biologically resolved in detail. The biological state variables of the present model are highly aggregated and little qualitative information about the biological compartment is produced. One exception is the distinction between the phytoplankton that does and does not need silicate.

How could more biological detail be included? A reasonable aim for the present model would be the inclusion of state variables that respond appropriately to deep water exchange. Such exchanges would probably result in a larger oxygenated habitat, a larger herbivore (*Calanus finmarchicus*), a shift in the composition of invertebrate carnivores, and pronounced diel vertical migrations. The separation of *C. finmarchicus* from the other herbivores would be justified by the body size and the generation time of 1 year (Aksnes & Magnesen, 1983). The diel vertical migrations of *C. finmarchicus* may reflect the significance of avoiding visual predators (such as the herring). The larger size makes the species more visible than other copepods such as *Paracalanus*, *Pseudocalanus* and *Temora* and the much longer generation time means that predation exposure becomes a higher risk than in the case of the other species. While physical forcing may be important for the shift in phytoplankton and zooplankton species composition, visual predation may be a key factor responsible for the shift in the vertical migrational pattern among the herbivores. The model of Clarke and Levy (1988) demonstrates visual predation as an explanation of the evolution of vertical migrational patterns, and their approach seems to recommend the implementation of the vertical migrations in simulation models of the present category.

Acknowledgements

This paper is based on scientific studies carried out in Lindåspollene by graduate and Dr scient. students at the University of Bergen, and by marine scientists from a number of Norwegian institutions. Many of them are referenced in the paper, but we take this opportunity to thank all the contributors of the field and laboratory data which have been used in the modelling. We wish particularly to acknowledge Mr Oddvar Dahl, Institute of Marine Research, for his support of the research project in Lindåspollene since it began in 1971. We thank Mr Leif Hestad who made the first attempts to implement a dynamic simulation model, Mr Poul Andersen who designed the basic structure of the Fortran code and Bergen Scientific Centre for providing excellent computer facilities. The research has been supported by the Norwegian Research Council for Science and Humanities (NAVF) and the Norwegian Fisheries Research Council (NFFR).

References

- Aksnes, D. L. & Magnesen, T. 1983 Distribution, development, and production of *Calanus finmarchicus* (Gunnerus) in Lindåspollene, western Norway, 1979. *Sarsia* **68**, 195–208.
- Aksnes, D. L. & Magnesen, T. 1988 A population dynamics approach to the estimation of four calanoid copepods in Lindåspollene, western Norway. *Marine Ecology Progress Series* **45**, 57–68.
- Aksnes, D. L., Magnesen, T. & Lie, U. 1985 Nutrient enrichment experiments in plastic cylinders and the implications of enhanced primary production in Lindåspollene, western Norway. *Sarsia* **70**, 45–58.
- Andersen, V. & Nival, P. 1988 A pelagic ecosystem model simulating production and sedimentation of biogenic particles: role of salps and copepods. *Marine Ecology Progress Series* **44**, 37–50.
- Andersen, V. & Nival, P. 1989 Modelling phytoplankton dynamics in an enclosed water column. *Journal of the Marine Biological Association of the United Kingdom* **69**, 625–646.
- Aure, J. N. 1972 Hydrografien i Lindåspollene. Unpubl. cand. real. thesis, University of Bergen, Norway, 121 pp.

- Banse, K. 1987 Clouds, deep chlorophyll maxima and the nutrient supply to the mixed layer of stratified water bodies. *Journal of Plankton Research* **9**, 1031–1036.
- Båmstedt, U. & Tande, K. 1988 Physiological responses of *Calanus finmarchicus* and *Metridia longa* (Copepoda: Calanoida) during the winter–spring bloom. *Marine Biology* **99**, 31–38.
- Clark, C. W. & Levy, D. A. 1988 Diel vertical migrations by sockeye salmon and the antipredation window. *American Naturalist* **131**, 271–290.
- Dahl, O., Østvedt, O. J. & Lie, U. 1973 An introduction to a study of the marine ecosystem and local herring stock in Lindåspollene. *Fiskeridirektoratets Skrifter Serie Havundersøkelser* **16**, 148–158.
- Denman, K. L. & Gargett, A. E. 1983 Time and space scales of vertical mixing and advection of phytoplankton in the upper ocean. *Limnology and Oceanography* **28**, 801–815.
- Eppley, R. W. 1972 Temperature and phytoplankton growth in the sea. *Fishery Bulletin* **70**, 1063–1085.
- Erga, S. R. 1990 The importance of external physical controls on vertical distribution of phytoplankton and primary production in fjords of western Norway. Dr scient. thesis, University of Bergen, 158 pp.
- Fasham, M. J. R., Holligan, P. M. & Hugh, P. R. 1983 The spatial and temporal development of the spring bloom in the Celtic Sea, April 1979. *Progress in Oceanography* **12**, 87–145.
- Hassel, A. 1980 Populasjonsdynamikk hos *Pseudocalanus elongatus* (Boeck) i Lindåspollene. Unpubl. cand. real thesis, University of Bergen, 83 pp.
- Hirche, H. J. 1983 Overwintering of *Calanus finmarchicus* and *Calanus helgolandicus*. *Marine Ecology Progress Series* **11**, 281–290.
- Jamart, B. M., Winter, D. F., Banse, K., Anderson, G. C. & Lam, R. K. 1977 A theoretical study of phytoplankton growth and nutrient distribution in the Pacific Ocean off the northwestern U.S. coast. *Deep Sea Research* **24**, 753–773.
- Jamart, B. M., Winter, D. F. & Banse, K. 1979 Sensitivity analysis of a mathematical model of phytoplankton growth and nutrient distribution in the Pacific Ocean off the northwestern U.S. coast. *Journal of Plankton Research* **3**, 267–290.
- Johannessen, A. 1983 Recruitment studies of herring (*Clupea harengus* L.). Dr scient. thesis, University of Bergen, Norway, 16 pp.
- Kremer, J. N. & Nixon, S. W. 1978 *A Coastal Marine Ecosystem. Simulation and Analysis*. Springer-Verlag, Berlin, 211 pp.
- Lehman, J. T. 1988 Algal biomass unaltered by food-web changes in Lake Michigan. *Nature* **332**, 537–538.
- Lännergren, C. 1975 Phosphate, silicate, nitrate and ammonia in Lindåspollene, a Norwegian landlocked fjord. *Sarsia* **59**, 53–66.
- Lännergren, C. 1976 Primary production in Lindåspollene, a Norwegian land-locked fjord. *Botanica Marina* **19**, 259–272.
- Lännergren, C. 1978 Phytoplankton production at two stations in Lindåspollene, a Norwegian land-locked fjord, and limiting nutrients studied by two kinds of bioassays. *Internationale Revue der Gesamten Hydrobiologie* **63**, 57–76.
- Lännergren, C. & Skjoldal, H. R. 1975 The spring phytoplankton bloom in Lindåspollene, a landlocked Norwegian fjord. Autotrophic and heterotrophic activities in relation to nutrients. In *Proceedings of the 10th European Symposium on Marine Biology, Volume 2* (Persoone, G. & Jaspers, E., eds). Universa Press, Belgium.
- Lie, U., Magnesen, T., Tunberg, B. & Aksnes, D. L. 1983 Preliminary studies on the vertical distribution of size-fractions in the zooplankton community in Lindåspollene, western Norway. *Sarsia* **68**, 65–80.
- Lie, U., Dahl, O. & Østvedt, O. J. 1978 Aspects of the life history of the local herring stock in Lindåspollene, western Norway. *Fiskeridirektoratets Skrifter Serie Havundersøkelser* **16**, 369–404.
- Magnesen, T. 1988 Vertical distribution of zooplankton in Lindåspollene, western Norway. Dr scient. thesis. University of Bergen, 147 pp.
- Magnesen, T., Aksnes, D. L. & Skjoldal, H. R. 1989a Fine-scale vertical structure of a summer zooplankton community in Lindåspollene, western Norway. *Sarsia* **74**, 115–126.
- Magnesen, T., Aadnesen, A. & Lie, U. 1989b Nutrient content in runoff water to Lindåspollene. IMB rapport no. 1. University of Bergen, 16 pp.
- McQueen, D. J., Johannes, M. R. S. & Post, J. R. 1989 Bottom-up and top-down impacts on freshwater pelagic community structure. *Ecological Monographs* **59**, 289–309.
- Northcote, T. G. 1987 Fish in the structure and function of freshwater ecosystems: a “top-down” view. *Canadian Journal of Fisheries and Aquatic Sciences* **45**, 361–379.
- Radach, G. & Maier-Reimer, E. 1975 The vertical structure of phytoplankton growth dynamics. A mathematical model. *Mémoires Société Royale des Sciences de Liège* **7**, 113–146.
- Riley, M. J. & Stefan, H. G. 1988 Minlake: a dynamic lake water quality simulation model. *Ecological Modelling* **43**, 155–182.
- Press, W. H., Flannery, B. P., Tevkolsky, S. A. & Vetterling, W. T. 1987 *Numerical Recipes*. Cambridge University Press, Cambridge.
- Sætre, R., Aure, J. & Ljøen, R. 1988 Wind effects on the lateral extension of the Norwegian Coastal Water. *Continental Shelf Research* **8**, 239–253.

- Scavia, D., Fahnenstiel, G. L., Evans, M. S., Jude, D. J. & Lehman, T. 1986 Influence of salmonine predation and water on long-term water quality trends in Lake Michigan. *Canadian Journal of Fisheries and Aquatic Sciences* **43**, 435–443.
- Scavia, D., Lang, D. A. & Kitchell, J. F. 1988 Dynamics of Lake Michigan plankton: a model evaluation of nutrient loading, competition, and predation. *Canadian Journal of Fisheries and Aquatic Sciences* **45**, 165–177.
- Skjoldal, H. R. & L  nnergren, C. 1978 The spring phytoplankton bloom in Lind  spollene, a landlocked Norwegian fjord. II. Biomass and activity of net and nanoplankton. *Marine Biology* **47**, 313–323.
- Skjoldal, H. R., Johannessen, P., Klinken, J. & Haldorsen, H. 1983 Controlled ecosystem experiment in Lind  spollene, western Norway, June 1979: comparison between the natural and two enclosed water columns. *Sarsia* **68**, 47–64.
- Skjoldal, H. R. & Wassmann, P. 1986 Sedimentation of particulate organic matter and silica during spring and summer in Lind  spollene, western Norway. *Marine Ecology Progress Series* **30**, 49–63.
- Slagstad, D. 1981 Modeling and simulation of physiology and population dynamics of copepods. Effects of physical and biological parameters. *Modeling, Identification and Control* **2**, 119–162.
- Slagstad, D. 1982 A model of phytoplankton growth-effects of vertical mixing and adaptation to light. *Modeling, Identification and Control* **3**, 111–130.
- Stigebrandt, A. & Wulff, F. 1987 A model for the dynamics of nutrients and oxygen in the Baltic proper. *Journal of Marine Research* **45**, 729–759.
- Steele, J. H. 1962 Environmental control of photosynthesis in the sea. *Limnology and Oceanography* **7**, 137–150.
- Taylor, A. H. 1988 Characteristic properties of models for the vertical distribution of phytoplankton under stratification. *Ecological Modelling* **40**, 175–199.
- Taylor, A. H., Farris, J. R. W. & Aiken, J. 1986 The interaction of physical and biological processes in a model of the vertical distribution of phytoplankton under stratification. In *Marine Interfaces Ecohydrodynamics* (Nihoul, J. C. J., ed.). Elsevier Oceanography Series, 42, Elsevier, Amsterdam, pp. 313–330.
- Wassmann, P. 1983 Sedimentation of organic and inorganic particulate material in Lind  spollene, a stratified, landlocked fjord in western Norway. *Marine Ecology Progress Series* **13**, 237–248.
- Winter, D. F., Banse, K. & Anderson, G. C. 1975 The dynamics of phytoplankton in Puget Sound, a fjord in the northwestern United States. *Marine Biology* **29**, 139–176.
- Wroblewski, J. S. 1983 The role of modeling in biological oceanography. *Ocean Science and Engineering* **8**, 245–285.